Lattice dynamics of thin ionic slabs. III. Application to GaAs slabs

G. Kanellis,* J. F. Morhange, and M. Balkanski
Laboratoire de Physique des Solides de l'Université Pierre et Marie Curie associé au Centre National de la Recherche Scientifique, 4 Place Jussieu, F-75230 Paris Cedex 05, France
(Received 15 March 1982; revised manuscript received 11 March 1983)

The lattice vibrations of thin slabs (up to 25 layers) of GaAs are calculated for zero wave vector, on the basis of a rigid-ion model fitted on the phonon dispersion curves of the infinite crystal. It is shown that all the modes, except the surface ones, fall on the branches of the dispersion curves of the infinite crystal, while the surface modes seem to be combinations of those missing near the zone-edge modes. Comparison is made with former calculations and the influence of the short-range interaction near the surfaces and that of possible macroscopic fields is discussed.

I. INTRODUCTION

Normal modes of vibrations of thin ionic slabs have been investigated theoretically by many authors,[1-9] mainly on the basis of a rigid-ion model, and the existence of surface modes have been well established. Jones and Fuchs[7] calculated the unretarded modes of a thin NaCl slab; they developed a theory for the infrared optical properties of ionic slabs and discussed previously published results on surface modes. Since most of the work mentioned above has been done on NaCl slabs a more substantial comparison is possible between their results. Benedek[9] calculated surface dispersion curves and phonon densities for thin ionic slabs on the basis of a breathing shell model using Green's-function formalism. This approach suitably extended proves to give very good results compared to those from direct calculations on thin slabs.

A very general approach to the effect of surfaces on the vibrational modes of crystalline solids is given by Feuchtwang[10] based on the assumption of finite-range interaction. Although in ionic crystals long-range electrostatic interaction is important, infinite-range forces arise only in the presence of a macroscopic field. Hence his results must be, in general, valid. Different features may appear to apply only to modes depending strongly on forces due to such fields. The influence of a macroscopic field on the vibrational modes of a slab will be discussed briefly in the last paragraph of Sec. IV.

Dispersion relations for surface modes are given by Fuchs and Kliewer[1] who found all long-wavelength optical modes of an ionic slab to have either TO or LO frequencies. Tong and Maradudin[3] treated in detail the case of a NaCl slab parallel to the (100) plane and pointed out the importance of some approximations made in the former work. Further comments on this point are given by Jones and Fuchs.[7] We also found the proper description of the short-range interaction between atoms near the surface to be of fundamental importance in calculating the correct frequencies of the surface modes.

Among the considerable experimental works on infrared absorption or Raman scattering on thin films and powders, which show vibrational states either between the TO and LO frequencies of the infinite crystal or below the TO frequency, we mention the infrared transmission and reflection measurements on thin (up to 68 μm) films on GaAS by Cochran *et al.*[11] and Fray *et al.*[12] They observed in a 25 μm thin film, lattice absorption on the TO and LO frequencies and also two other strong peaks on frequencies lying between these two. Each of those peaks seems to consist of three or four fine-structure peaks. These features are attributed to the size, shape, and orientation of the specimens used.

Raman spectra on laser-annealed GaAs (Ref. 13) show a gradual transition from the amorphous spectrum to the crystalline one involving a continuous variation of degree of order versus the annealing density energy. The above experimental results and also analogous results on other materials reveal the need for a complete calculation of infrared and Raman spectra of small crystallites in order to justify the hypothesis of size effects.

In the present paper we report on calculations of vibrational modes of thin GaAs slabs parallel to $(11\bar{1})$ planes, on the basis of a rigid-ion model. This model has been used by Kunc[14] to fit measured phonon dispersion curves, hence our results are directly

comparable to the ones of an infinite crystal. The long-range interaction has been calculated in a former paper[15] referred to as paper II.

In the next section we briefly review the equations of motion and the resulting dynamical matrix to be solved. In the third section we describe in short the rigid-ion model used for the calculation and the procedure applied to calculate the short-range interaction of atoms lying near the surfaces. Finally, in the last section we describe the results obtained and we discuss them in comparison with other results.

II. EQUATIONS OF MOTION AND DYNAMICAL MATRIX

We consider a crystal slab of zinc-blende structure (particularly GaAs) parallel to the $(11\bar{1})$ plane. Choosing a Cartesian coordinate system $Ox_1x_2x_3$, whose axes are parallel to the edges of the cubic fcc unit cell and its origin on an ion site (for instance, a Ga site), the primitive translation vectors are

$$\begin{bmatrix}\vec{a}_1\\ \vec{a}_2\\ \vec{a}_3\end{bmatrix}=\frac{a}{2}\begin{bmatrix}0&1&1\\1&0&1\\1&1&0\end{bmatrix}\begin{bmatrix}\vec{x}_{01}\\ \vec{x}_{02}\\ \vec{x}_{03}\end{bmatrix}, \tag{1}$$

where a is the lattice constant. Vectors $\vec{a}_1$ and $\vec{a}_2$ lie on the plane $(11\bar{1})$ while $\vec{a}_3$ lies out of it.

The equations of motion for a lattice are[16]

$$m_\kappa \ddot{u}_\alpha(l,\kappa)=-\sum_{l',\kappa'}\sum_{\beta}\phi_{\alpha\beta}(l,\kappa;l',\kappa')u_\beta(l',\kappa'), \tag{2}$$

where m_κ is the mass of the κth kind of ion, $u_\alpha(l,\kappa)$ is the αth Cartesian component of the displacement from the equilibrium position, $\phi_{\alpha\beta}(l,\kappa;l',\kappa')$ are the atomic force constants, and $l=(l_1,l_2,l_3)$ labels the unit cells.

Applying cyclic boundary conditions along the directions $\vec{a}_1$ and $\vec{a}_2$ [on the infinite $(11\bar{1})$ plane] we put

$$u_\alpha(l,\kappa)=\frac{v_\alpha(l_3,\kappa)}{m_\kappa^{1/2}}\exp[-i\omega t+2\pi i\vec{y}\cdot\vec{x}(l,\kappa)], \tag{3}$$

where $\vec{y}$ is a two-dimensional wave vector. Equation (2) becomes

$$\omega^2 v_\alpha(l_3,\kappa)=\sum_{l'_3,\kappa'}\sum_{\beta}D_{\alpha\beta}(l_3,\kappa;l'_3\kappa'\mid\vec{y})v_\beta(l'_3\kappa'), \tag{4}$$

where

$$D_{\alpha\beta}(l_3,\kappa;l'_3,\kappa'\mid\vec{y})=\sum_{l'_1,l'_2}\frac{\phi_{\alpha\beta}(l,\kappa;l',\kappa')}{(m_\kappa m'_\kappa)^{1/2}}\times\exp[2\pi i\vec{y}\cdot\vec{x}(l,\kappa;l'\kappa')] \tag{5}$$

are the elements of the $6N\times 6N$ dynamical matrix (N is the number of layers in the slab). Since no periodic boundary condition is used along the finite dimension, any further reduction of the dynamical matrix will be likely possible only from symmetry considerations.

It has been shown[17] that for the above chosen orientation of the slab one can use a new coordinate system $Ox'_1x'_2x'_3$, related to the old one associated with the crystallographic unit cell, by the transformation

$$\begin{bmatrix}\vec{x}'_{01}\\ \vec{x}'_{02}\\ \vec{x}'_{03}\end{bmatrix}=\frac{1}{\sqrt{6}}\begin{bmatrix}-\sqrt{3}&\sqrt{3}&0\\1&1&2\\\sqrt{2}&\sqrt{2}&-\sqrt{2}\end{bmatrix}\begin{bmatrix}\vec{x}_{01}\\ \vec{x}_{02}\\ \vec{x}_{03}\end{bmatrix}, \tag{6}$$

whose Ox'_1 and Ox'_2 axes are coplanar with the slab, while axis Ox'_3 is perpendicular to it. Since it is always possible to find such a coordinate system, whatever the orientation of the slab might be, let us denote the corresponding transformation matrix by $\underline{H}$ [in the present case H is the 3×3 unitary matrix used in Eq. (6)].

With the use of transformation H and the representation of the space group G of the three-dimensional structure with respect to the old coordinate system, one can construct a new space group G' appropriate for the two-dimensional structure of the slab, by transforming the representation of G to the new coordinate system and by picking up those elements which act only parallel to the plane of the slab.

Group G' can then be used to provide the form of the force-constant matrices and the relations between the elements of the dynamical matrix. In the present case and for wave vector $\vec{y}=\vec{0}$, we find that the interaction between the plane lattices assumes the general form

$$\underline{D}(l_3,\kappa;l'_3,\kappa')=\begin{bmatrix}A&B&-B\\B&A&-B\\-B&-B&A\end{bmatrix} \tag{7}$$

in the old coordinate system $Ox_1x_2x_3$, while in the system $Ox'_1x'_2x'_3$ it takes the form

$$\underline{D}'(l_3,\kappa;l'_3,\kappa')=\begin{bmatrix}A-B&0&0\\0&A-B&0\\0&0&A+2B\end{bmatrix} \tag{8}$$

through the transformation

$$\underline{D}'(l_3,\kappa;l_3'\kappa')=\underline{H}\,\underline{D}(l_3,\kappa;l_3',\kappa')\underline{H}^{-1}\,. \tag{9}$$

The form of Eq. (8) implies that for the so-chosen orientation of the slab, the solutions of Eq. (4) fall into two groups, one doubly degenerate consisting of the in-plane solutions (x-y modes) and one nondegenerate consisting of the out-of-plane solutions (z modes).

The matrix whose elements are defined by Eq. (5) expresses the interaction between plane lattices and has to be calculated on the basis of some model. In the next section we give a brief description of the applied rigid-ion model. Since both short- and long-range forces are taken into account, it is customary to consider the dynamical matrix as consisting of two parts, the short-range (sr) and the Coulomb parts;

$$\underline{D}(l_3,\kappa;l_3',\kappa')=\underline{D}^{\mathrm{sr}}(l_3,\kappa,l_3',\kappa)+\underline{D}^{C}(l_3,\kappa;l_3',\kappa)\,. \tag{10}$$

The form of the interaction matrices between the plane lattices of the slab for zero wave vector, is given in the Appendix.

The Coulomb part can be expressed in terms of the Q coefficients calculated in paper II [Eqs. (10) and (14)], and for the general wave vector it assumes the form

$$D^{C}_{\alpha\beta}(l_3\kappa;l_3'\kappa'\mid\vec{\gamma})=\delta_{l_3l_3'}\delta_{\kappa\kappa'}\frac{\xi_\kappa}{m_\kappa}\times\sum_{l_3'',\kappa''}\xi_{\kappa''}Q_{\alpha\beta}(l_3,\kappa;l_3''\kappa''\mid\vec{0})-\frac{\xi_\kappa\xi_{\kappa'}}{(m_\kappa m_{\kappa'})^{1/2}}Q_{\alpha\beta}(l_3,\kappa;l_3',\kappa'\mid\vec{\gamma})\,, \tag{11}$$

where ξ_κ is the charge fraction attributed to ion κ. Values of the Q coefficients for zero wave vector are also given in the Appendix (Table I).

TABLE I. Values of the Coulomb coefficient β [in units of $(Ze)^2/v_\beta$].

κ	κ'	l'	β
1	2	0	−5.591 35
1	1	1	−0.143 41
1	2	1	−0.033 49
2	1	1	1.437 62
2	2	1	−0.143 41
1	1	2	−0.000 40
1	2	2	0.000 18
2	1	2	−0.001 75
2	2	2	−0.000 40

III. THE MODEL

In the present case we use the rigid-ion model (RIM) developed and applied to several binary compounds of the zinc-blende structure by Kunc.[14] Apart from the effective charge q^* the model parameters are ten tensorial force constants, A and B for first-neighbor central and noncentral interaction, C_1, D_1, E_1, F_1, C_2, D_2, E_2, and F_2, for second-neighbor central and noncentral interaction, for the two different kinds of ions.

All of the above parameters have been fitted to experimentally known phonon dispersion curves, the elastic constants, and the piezoelectric constant. In order to use the above model in the case of a slab the following adaptations have to be made:

(a) Long-range forces have to be recalculated on the basis of new suitable formulas as already mentioned.

(b) Short-range interaction of the near-the-surface atoms has to be modified, so as to take the missing ions into account. For the short-range part of the dynamical matrix the following procedure has been followed. From the ten fitted tensorial force constants, the values of a set of ten valence force field (VFF) force constants are deduced, namely the ξ, λ, ρ, μ, σ, ν, k_θ, k_θ', k_{rr}, and k_{rr}' according to the following model for the potential energy:

$$\Phi=r_0\xi\sum_{\text{Ga-As}}\Delta r_{ij}+\frac{\lambda}{2}\sum_{\text{Ga-As}}(\Delta r_{ij})^2+r_1\rho\sum_{\text{Ga-Ga}}\Delta r_{ik}+\frac{\mu}{2}\sum_{\text{Ga-Ga}}(\Delta r_{ik})^2+r_1\sigma\sum_{\text{As-As}}\Delta r_{jl}+\frac{\nu}{2}\sum_{\text{As-As}}(\Delta r_{jl})^2+\frac{k_\theta r_0^2}{2}\sum_{\text{As-Ga-As}}(\Delta\theta_{jil})^2+\frac{k_\theta' r_0^2}{2}\sum_{\text{Ga-As-Ga}}(\Delta\theta_{ijk})^2+\frac{k_{rr'}}{2}\sum_{\text{As-Ga-As}}\Delta r_{ji}\Delta r_{il}+\frac{k'_{rr'}}{2}\sum_{\text{Ga-As-Ga}}\Delta r_{ij}\Delta r_{jk}\,, \tag{12}$$

where r_0 and r_1 are the first- and second-nearest-neighbor distances, respectively.

The interaction of the near-the-surface ions is calculated on the basis of the above VFF model. It should be noted that the ten VFF parameters are not independent, but have to fulfill the equilibrium condition. For the given values of the tensorial force constants this condition does not hold. Hence we

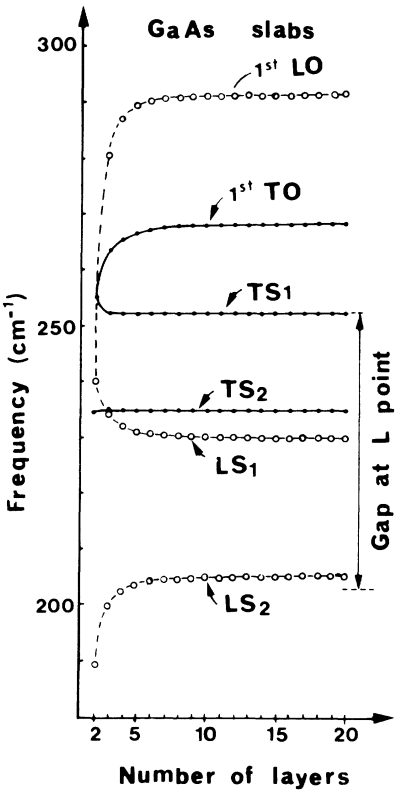

FIG. 1. Variation of the frequencies of six modes vs the thickness of the slab.

decompose the tensorial force constants into the VFF parameters disregarding this condition.

By so doing, only the interaction of atoms lying near the surfaces may be influenced. Since the correct description of the above interaction is of critical importance in calculating the surface mode frequencies, one needs a faithful VFF model in order to obtain unambiguous results for these modes. In the next section we comment on the results based on the above consideration and on those obtained when the short-range interaction of surface atoms is considered to be the same as for atoms in the interior of the slab.

IV. RESULTS AND DISCUSSION

We have calculated the frequencies and the eigenvectors for thin slabs of GaAs oriented parallel to the $(11\bar{1})$ plane with thicknesses from 2 up to 25 cells (10—130 Å thick) for zero (two-dimensional) wave vector.

The main feature displayed by the solutions is that, by increasing the number of layers of the slab (i.e., its thickness) all of the solutions tend rapidly to certain limits, while the new solutions appearing in each thicker slab are interpolated between the solutions of the thinner one. For a slab 20 layers thick all the frequencies are within 1% of their limits.

In Fig. 1 we show the variation of the frequencies of six modes versus the thickness of the slabs: the highest-frequency z mode (first LO), the highest-frequency x-y mode (first TO), and four surface modes, i.e., two surface x-y modes ($TS1$ and $TS2$) and two surface z modes ($LS1$ and $LS2$). We see that the surface modes $TS1$ and $TS2$ have practically constant frequency for any slab as thin as three layers, while the frequencies of the rest of the modes tend very rapidly to their limiting values.

The two-dimensional Brillouin zone corresponding to the slab structure is a section through the center of the three-dimensional zone of the fcc lattice, perpendicular to the Λ direction $(-\xi, -\xi, \xi)$. Comparing the frequencies of the above modes with the frequencies of the modes belonging to the dispersion branches of the Λ direction of the infinite crystal, we find that the first LO and first TO modes tend to have frequencies equal to those of the LO and TO modes of the Γ point of the infinite structure, respectively. The surface mode $TS1$ has a frequency almost equal to the TO mode at the L point, while modes $TS2$, $LS1$, and $LS2$ have frequencies which fall into the gap at the L point of the infinite crystal.

Before making any further comments on the surface modes and on the rest of the modes, we will turn our attention to the eigenvectors. For a GaAS slab N layers thick, there are $2N$ x-y modes, which are doubly degenerate (the transverse modes), and $2N$ z modes (the longitudinal ones). From the $2N$ modes in each configuration, N are optical and the remaining N are acoustic. Among the N optical modes in each case there are two whose amplitudes decay exponentially along the finite dimension of the slab, from the one surface to the other, and are therefore called surface modes. For wave vectors different from zero the so-called Rayleigh waves[16] appear, among the acoustic modes. For each optic mode m we construct the difference of the reduced displacements,

$$f_m^{\mathrm{op}}(l_3)=\frac{u(l_3,1\mid m)}{\sqrt{M_1}}-\frac{u(l_3,2\mid m)}{\sqrt{M_2}}\ , \tag{13}$$

where 1 denotes the Ga atom, 2 the As atom, l_3 numbers the layers of the slab, and M is the mass. Accordingly, for the acoustic modes, we construct the sum of the same quantities.

$$f_m^{\mathrm{ac}}(l_3)=\frac{u(l_3,1\mid m)}{\sqrt{M_1}}+\frac{u(l_3,2\mid m)}{\sqrt{M_2}}\ . \tag{14}$$

In Fig. 2 we plot $f_m^{\mathrm{op}}(l_3)$ and $f_m^{\mathrm{ac}}(l_3)$ vs $z=l_3,a_\perp$,

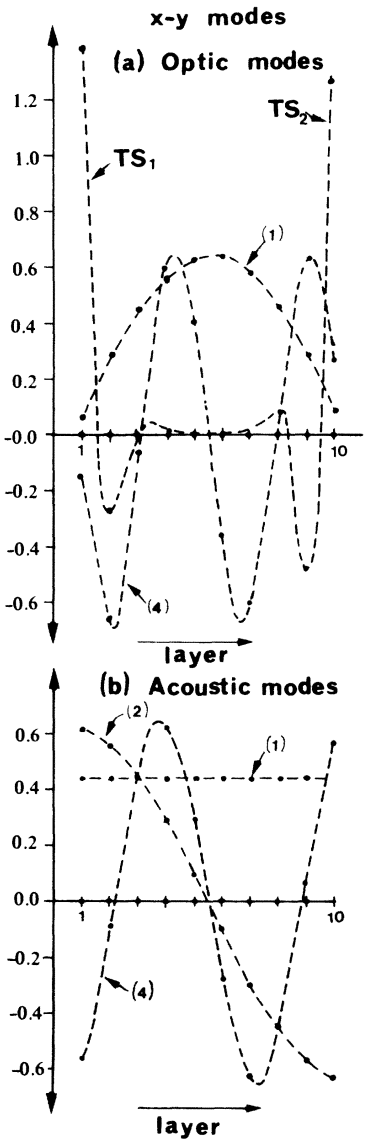

FIG. 2. For a slab of ten layers: (a) Relative reduced ionic displacements for some x-y optic modes. Numbering starts with the mode of highest frequency. (b) Sum of reduced ionic displacements for some x-y acoustic modes. Numbering starts with the zero-frequency mode.

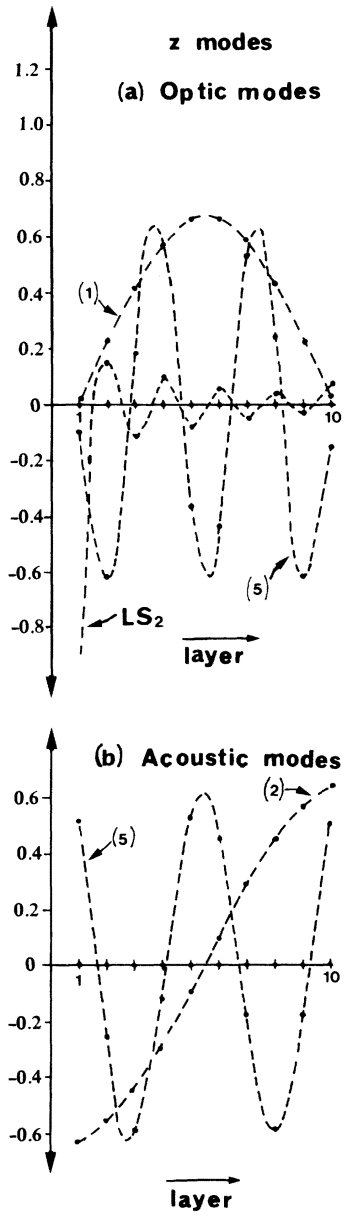

FIG. 3. For a slab of ten layers: (a) Relative reduced ionic displacements for some z optic modes. Numbering starts with the mode of highest frequency. (b) Some of reduced ionic displacements for some z acoustic modes. Numbering starts with the zero-frequency mode.

the coordinate along the finite dimension of the slab, for some x-y modes (transverse modes), and in Fig. 3 we plot the same functions for some z modes (longitudinal). It is evident from these figures that all the optic modes, except the surface ones, can almost be described (neglecting the sign) as

$$f_m^{\mathrm{op}}(z)\simeq\frac{2}{\sqrt{N}}\sin\frac{m\pi z}{L}\ , \tag{15}$$

where L is the thickness of the slab, while the acoustic modes can be described as

$$f_m^{\mathrm{ac}}(z)\simeq\frac{2}{\sqrt{N}}\cos\frac{(m-1)\pi z}{L} \tag{16}$$

($m=1,2,\ldots,N$, numbers the optic modes starting from the highest-frequency one and the acoustic modes starting from the zero-frequency one).

We note that the above simple trigonometric expressions do not describe exactly the functions of the displacement defined by Eqs. (13) and (12), but rath-

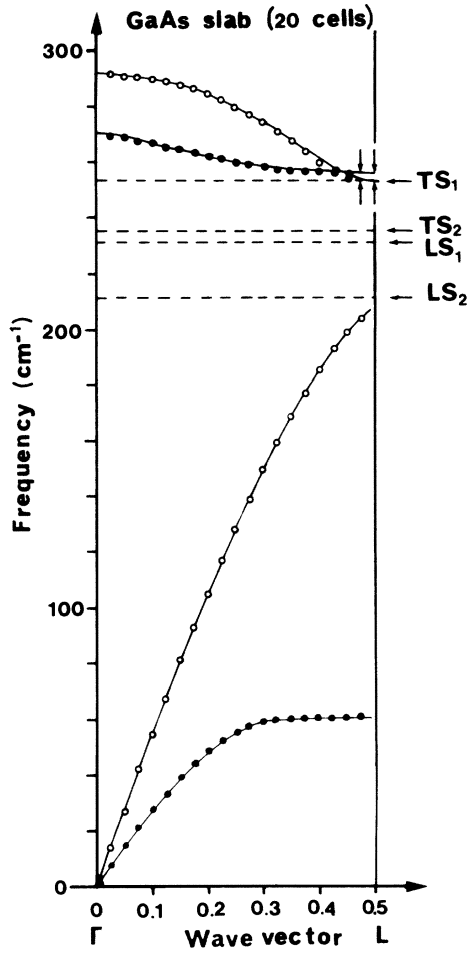

FIG. 4. Phonon dispersion curves of GaAs along the Λ direction (solid lines). x-y modes (solid circles) and z modes (open circles) for a slab of 20 layers thick. Broken lines show the position of surface modes. The positions of TO and LO missing modes near and on the zone boundary are shown by arrows.

er, give a good picture of what these functions look like. Moreover, although the functions sketched in Figs. 2 and 3 refer to a slab ten layers thick, the picture is the same for slabs of any thickness.

From Eqs. (15) and (16) we see that there is an implicit dependence of the modes on a wave vector along the finite dimension of the slab, although such an assumption has not been made. All the modes, except the surface ones, on which we will comment later on, seem to be characterized by the values of a wave vector

$$y_z = n\frac{\pi}{L} . \tag{17}$$

There is no optic mode with $n=0$, i.e., there is no mode of infinite wavelength. Since the surface modes cannot be described by the same function f_m^{op}, only $N-2$ optic modes could be attributed to the wave vectors of Eq. (17). On the other hand, all the N acoustic modes can be regarded as corresponding to some wave vector y_z. We should note that the solution of zero frequency for $y_z=0$ has been imposed by using relation (A5) when calculating the self-terms of the dynamical matrix.

According to the above observations, we plot in Fig. 4 the dispersion curves of GaAs along the Λ direction, as they have been calculated by Kunc[14] on the basis of the same model and we put on the same graph the solutions for a slab 20 layers thick. We have chosen this thickness where each solution has reached its limit within less than 1%. Acoustic modes start from zero wave vector, while optic modes start from wave vector equal to 0.5/20. We see that all the modes, except the surface ones, fall on the corresponding branches: x-y modes on the transverse branches and z modes on the longitudinal ones. There are four optic modes missing. Instead there are four surface modes shown by dotted lines on the graph along the zonewidth, although they seem to belong to a value of the wave vector very close to the zone boundary. Hence we conclude that the surface modes could be regarded as superpositions of the missing optical modes, and perhaps the corresponding acoustic modes of the zone edge, in each configuration (transverse or longitudinal). The longitudinal surface modes (z modes), considered as being superpositions of modes of higher frequency, appear to have lower frequencies than the transverse ones. They also show considerably less decay along the finite dimension of the slab. Both of these features could be explained, qualitatively at the moment, by the weaker short-range forces near the surfaces and by the assumption that these modes are strongly damped by the long-range forces. We should note at this point that the slowest convergence of the frequencies to their limiting values, with increasing thickness of the slab, is observed for the longitudinal modes of shorter wavelength (wave vector near the zone edge). Indeed, the frequencies of the surface modes depend very strongly on the short-range forces assumed for the surface layers. If we restore on these layers the same short-range forces as for the rest of the slab, then all the modes, except the surface ones, tend faster to the same limiting frequencies. The surface modes have higher limits as follows: The $TS1$ mode, 253.3 cm^{-1} (instead of 252.5 cm^{-1}), the $TS2$ mode, 247.3 cm^{-1} (instead of 235 cm^{-1}), the $LS1$ mode, 250.7 cm^{-1} (instead of 230.7 cm^{-1}), and the $LS2$ mode, 249.6 cm^{-1} (instead of 210.5 cm^{-1}). We see that the longitudinal surface modes have a much stronger dependence on the short-range forces assumed for the sur-

face layers, but still at least one of them should have higher frequency than the transverse modes if no damping due to long-range forces was existing. Hence the correct description of the short-range forces near the surfaces is of critical importance in calculating the surface mode frequencies. Of course, the eigenvectors are also influenced by the change of the forces near the surface, in particular the eigenvectors of the longitudinal modes, but they retain their main features. Stronger forces between the surface layers result in deeper penetration of those modes in the slab.

On the basis of the above observations it is clear that the continuum of frequencies for "bulk" modes obtained by several authors when calculating solutions for different wave vectors on the plane of a slab, is the projection of the dispersion surfaces of the infinite crystal on the two-dimensional Brillouin zone appropriate for the slab. Comparing our results with those of Tong and Maradudin,[3] who calculated the solutions for a slab of NaCl parallel to (001) plane, we could note the following: The frequency of the transverse surface mode in NaCl, lying just below the lower limit of the "bulk" optical modes, is in agreement with our results. The near degeneracy of both pairs of surface modes they found can be explained by the fact that the two surfaces of the NaCl slab in the above orientation are completely equivalent. Moreover, the thickness of this slab is an integer multiple of the lattice constant, while in our case it is not. This feature may be of importance when superimposing plane waves, due to the phase difference it may introduce. As far as it concerns the higher-frequency surface modes for zero wave vector in the case of the NaCl slab, they can be considered as unlocalized surface modes whose wave vector perpendicular to the plane of the slab can assume values either at the center or at the zone boundary[10] in the present case. The corresponding modes in our case are of the same type as those found by Wallis.[18] This difference may be due to the fact that the NaCl slab consists of identical "neutral" planes.

Fuchs and Kliewer[1] treated the case of long-wave optical vibrations in a slab in the electrostatic approximation. Apart from the influence on their results due to approximations concerning the short-range forces near the surfaces and the replacement of infinite sums by integrals, which have been discussed by Tong and Maradudin,[3] we would like to note that their results for "bulk" modes concern those modes which lie on the corresponding branches but very near to the Γ point. Hence for a thick slab there are many modes which have the zone-center TO and LO frequencies with small wave vectors $m\pi/L$. For optic modes we have found only the sine dependence of the displacements with odd and even values of m. Their point, that this dependence is such that there are exactly m half waves across the thickness of the slab, is correct even for very thin slabs and for the acoustic modes also. The quantization of the wave vector along the finite dimension is of course the same for all dispersion branches.

The surface modes found by these authors reduce, for zero wave vector on the plane of the slab, in unlocalized surface modes, corresponding to zone-center modes of the infinite crystal. It has been shown by Feuchtwang[10] that these modes are a special case of bulk modes. Since the above authors treated the case of long waves, these modes may be the only ones which, for finite wave vectors ($\neq 0$) on the plane of the slab, became surface modes. Lucas[4] and Jones and Fuchs[7] attribute the above behavior of these modes to the neglect of the changes of the forces acting on atoms near the surfaces. The results of the latter author at $\vec{y}=\vec{0}$ are in agreement to those of Lucas, and Tong and Maradudin, as to the number and type of surface modes.

A final remark concerns the possible influence of macroscopic fields. We have shown in paper II that vibrations involving ionic displacements perpendicular to the plane of the slab give rise to a potential difference between its two surfaces. This potential does not influence the vibrations of a free slab, except if it results in additional surface charges, or if the slab is considered in some polarizable environment. In such cases, assuming complete compensation of the above potential, all the frequencies of the z modes tend slower to the same limits, while an additional phase difference is introduced in the displacements of atoms in neighboring cells. This phase difference moves all the optic modes one step toward the zone boundary. Hence for a slab thicker than ten layers, the relative displacements show the same pattern as described by Eq. (15), but now modes with $m=0$, $m=1$, and $m=N-1$ are missing.

APPENDIX

The form of force-constant matrices (interaction between individual ions) for the zinc-blende structure is the following:

$$\underline{\Phi}(l,1;l,2)=\begin{bmatrix} A & B & B \\ B & A & B \\ B & B & A \end{bmatrix}, \quad \underline{\Phi}(l,2;l',1)=\begin{bmatrix} A & B & -B \\ B & A & -B \\ -B & -B & A \end{bmatrix},$$
$$\underline{\Phi}(l,1;l',1)=\begin{bmatrix} C_1 & D_1 & E_1 \\ D_1 & C_1 & E_1 \\ -E_1 & -E_1 & F_1 \end{bmatrix}, \quad \underline{\Phi}(l,2;l',2)=\begin{bmatrix} C_2 & D_2 & E_2 \\ D_2 & C_2 & E_2 \\ -E_2 & -E_2 & F_2 \end{bmatrix}, \tag{A1}$$

where $l=(l_1,l_2,l_3)$ and $l'=(l_1,l_2,l_3+1)$.

For the surface layers $l_0=(l_1,l_2,1)$ and $l_N=(l_1,l_2,N)$ the force-constant matrices in the present case take the form

$$\underline{\Phi}(l_0,1;l_0,2)=\begin{bmatrix} A_1 & B_1 & B_1 \\ B_1 & A_1 & B_1 \\ B_2 & B_2 & A_2 \end{bmatrix}, \quad \underline{\Phi}(l_N,1;l_N,2)=\begin{bmatrix} A_3 & B_3 & B_4 \\ B_3 & A_3 & B_4 \\ B_3 & B_3 & A_5 \end{bmatrix}. \tag{A2}$$

The decomposition of the tensorial force constants into parameters of the VFF model used can be found in Ref. 14 for all interactions, except the ones between ions in the surface layers, which are listed below:

$$A_1=A-k_{rr'}/6, \quad A_2=A+4k_\theta/3+k_{rr'}/6, \quad A_3=A-k'_{rr'}/6, \quad A_4=4k'_\theta/3+k'_{rr'}/6,$$
$$B_1=B-k_{rr'}/6, \quad B_2=B-2k_\theta/3+k_{rr'}/6, \quad B_3=B-k'_{rr'}/6, \quad B_4=B-2k'_\theta/3+k'_{rr'}/6. \tag{A3}$$

The interaction matrices for plane lattices for zero wave vector (submatrices of the dynamical matrix) assume the following forms (with $l'_3=l_3+1$):

$$\underline{D}(l_3,1;l_3,2)\sim\begin{bmatrix} 3A & -B & B \\ -B & 3A & B \\ B & B & 3A \end{bmatrix}, \quad \underline{D}(l_3,2;l'_3 1)\sim\begin{bmatrix} A & B & -B \\ B & A & -B \\ -B & -B & A \end{bmatrix}, \tag{A4a}$$

$$\underline{D}(l_3,1;l'_3,1)\sim\begin{bmatrix} 2C_1+F_1 & D_1 & -D_1 \\ D_1 & 2C_1+F_1 & -D_1 \\ -D_1 & -D_1 & 2C_1+F_1 \end{bmatrix}, \quad \underline{D}(l_3,2;l'_3,2)\sim\begin{bmatrix} 2C_2+F_2 & D_2 & -D_2 \\ D_2 & 2C_2+F_2 & -D_2 \\ -D_2 & -D_2 & 2C_2+F_2 \end{bmatrix}. \tag{A4b}$$

Self terms, for zero wave vector, are calculated on the basis of the equation[16]

$$\sum_{l',\kappa'}\Phi_{\alpha\beta}(l\kappa;l'\kappa')=0. \tag{A5}$$

The corresponding interaction matrices for planes of the surface layers ($l_3=1$ and $l_3=N$) take the form

$$\underline{D}(1,1;1,2)\sim\begin{bmatrix} 2A_1+A_2 & -B_2 & B_2 \\ -B_2 & 2A_1+A_2 & B_2 \\ B_2 & B_2 & 2A_1+A_2 \end{bmatrix}, \quad \underline{D}(N,1;N,2)\sim\begin{bmatrix} 2A_3+A_4 & -B_4 & B_4 \\ -B_4 & 2A_3+A_4 & B_4 \\ B_4 & B_4 & 2A_3+A_4 \end{bmatrix}. \tag{A6}$$

All the Coulomb interaction matrices assume for zero wave vector the form

$$\underline{Q}(0,\kappa;l',\kappa')=\begin{bmatrix} 0 & \beta & -\beta \\ \beta & 0 & -\beta \\ -\beta & -\beta & 0 \end{bmatrix}. \tag{A7}$$

The values of β are given in Table I for $l'=0$, 1, and 2. All more distant interactions are less than 10^{-5} [in units of $(Ze)^2/v_\alpha$].

*Permanent address: First Laboratory of Physics, University of Thessaloniki, Thessaloniki, Greece.

[1]R. Fuchs and K. L. Kliewer, Phys. Rev. 140, A2076 (1965).
[2]R. Englman and R. Ruppin, J. Phys. C 1, 614 (1967).
[3]S. Y. Tong and A. A. Maradudin, Phys. Rev. 181, 1318 (1968).
[4]A. A. Lucas, J. Chem. Phys. 48, 3156 (1968).
[5]V. V. Bruksin and Yu. A. Firsov, Fiz. Tverd. Tela (Leningrad) 11, 2167 (1969) [Sov. Phys.—Solid State 11, 1751 (1970)].
[6]R. E. Allen, G. P. Alldredge, and F. W. de Wette, Phys. Rev. B 4, 1648 (1971).
[7]W. E. Jones and R. Fuchs, Phys. Rev. B 4, 3581 (1971).
[8]W. E. W. Ludwig, Jpn. J. Appl. Phys. Suppl. 2, 879 (1974).
[9]G. Benedek, Surf. Sci. 61, 603 (1976).
[10]T. E. Feuchtwang, Phys. Rev. 155, 731 (1967).
[11]W. Cochran, S. J. Fray, F. A. Johnson, J. E. Quarrington, and N. Williams, J. Appl. Phys. Suppl. 32, 2102 (1961).
[12]S. J. Fray, F. A. Johnson, J. E. Quarrington, and N. Williams, Proc. Phys. Soc. London 77, 215 (1961).
[13]J. F. Morhange, G. Kanellis, and M. Balkanski, J. Phys. Soc. Jpn. Suppl. A 49, 1295 (1980).
[14]K. Kunc, Ann. Phys. (Paris) 8, 319 (1973-74).
[15]G. Kanellis, J. F. Morhange, and M. Balkanski, preceding paper, Phys. Rev. B 28, 3398 (1983).
[16]A. A. Maradudin, E. W. Montroll, G. H. Weiss, and I. P. Ipatova, *Theory of Lattice Dynamics in the Harmonic Approximation,* Supplement 3 of *Solid State Physics* (Academic, New York, 1971).
[17]G. Kanellis, J-F. Morhange, and M. Balkanski, Phys. Rev. B 21, 1543 (1980).
[18]R. F. Wallis, Phys. Rev. 105, 540 (1957).